Inorganic Chemistry

Article

pubs.acs.org/IC

Nonemployed Simple Carboxylate Ions in Well-Investigated Areas of Heterometallic Carboxylate Cluster Chemistry: A New Family of $\{Cu^{II}_4Ln^{III}_8\}$ Complexes Bearing *tert*-Butylacetate Bridging Ligands

Despina Dermitzaki,[†] Catherine P. Raptopoulou,[‡] Vassilis Psycharis,[‡] Albert Escuer,[§] Spyros P. Perlepes,*[,†] and Theocharis C. Stamatatos*[,∥]

[†]Department of Chemistry, University of Patras, 265 04 Patras, Greece

[‡]Institute of Nanoscience and Nanotechnology, NCSR "Demokritos", 15310 Aghia Paraskevi, Attikis, Greece

[§]Departament de Quimica Inorganica, Universitat de Barcelona, Diagonal 645, 08028 Barcelona, Spain

[∥]Department of Chemistry, Brock University, L2S 3A1 St. Catharines, Ontario, Canada

Supporting Information

ABSTRACT: The first use of *tert*-butylacetate as bridging ligand in 3d/4f-metal cluster chemistry, in conjunction with the versatile chelate ligand pyridine-2,6-dimethanol, has afforded a new family of $[Cu_4Ln_8(OH)_6(NO_3)_2(O_2CCH_2Bu^t)_{16}(pdm)_4]$ clusters with unprecedented structures and slow magnetization relaxation for the $\{Cu^{II}_4Dy^{III}_8\}$ member. The molecular structure of representative complex **1** consists of a $\{Cu^{II}_4Gd^{III}_8\}$ cage-like cluster built from two $\{CuGd_3\}$ cubanes which are linked to each other and to two {CuGd} subunits on opposite sides through two $\eta^2{:}\eta^2{:}\eta^2{:}\mu_5$ NO_3^- ions. The metal ions are additionally bridged by μ_3-OH^-, μ_3-OR^-, and μ-OR^- groups to give an overall $[Cu_4Gd_8(\mu_5\text{-}NO_3)_2(\mu_3\text{-}OH)_6(\mu_3\text{-}OR)_2(\mu\text{-}OR)_8]^{14+}$ core. Peripheral ligation about the core is provided by the N,O,O-chelating part of the pdm^{2-} groups and, more impressively, by the oxygen atoms of 16 bridging $Bu^tCH_2CO_2^-$ ligands; the latter are arranged into five classes, adopting a total of six different binding modes with the metal centers. The combined work demonstrates the ligating flexibility of *tert*-butylacetate ion and its usefulness in the synthesis of new 3d/4f-metal cluster compounds.

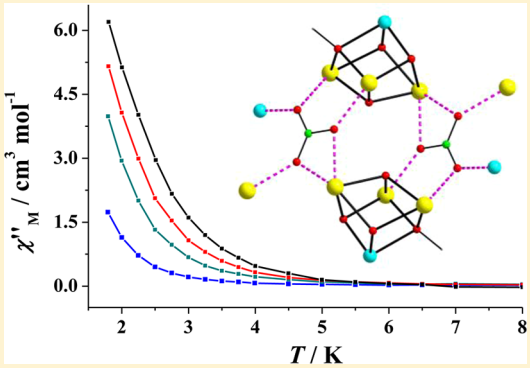

INTRODUCTION

Carboxylate ions (RCO_2^-; R = various) are among the most widely used bridging ligands in homometallic 3d- and 4f-metal cluster chemistry, as well as in heterometallic systems containing both 3d- and 4f-metal ions.[1] Owing to their relatively hard O donor atoms, carboxylates are capable of bridging up to five borderline-to-hard metal ions, thus fostering the metals' aggregation into a polymetallic motif and simultaneously blocking the extensive polymerization due to their chelating/terminal ability. Hence, over the last two decades or so, carboxylate groups have provided the means of obtaining beautiful new cluster compounds with aesthetically pleasing structures and interesting magnetic[1] and/or optical properties.[2]

In the field of molecular magnetism, the interest mainly stems from the ability of polynuclear, paramagnetic metal clusters to stabilize appreciable spin ground-state (S) values which, in addition to the presence of a significant magneto-anisotropy (as reflected in a large and negative zero-field splitting parameter, D), are the basic requirements for a molecular species to exhibit single-molecule magnet (SMM) behavior.[3] Fairly large S values are known to result from ferromagnetic exchange interactions between thoroughly chosen 3d- and 4f-metal ions (i.e., Cu^{II} and Gd^{III} ions).[4] When the f-block ions are also highly anisotropic (i.e., Dy^{III}), slow magnetization relaxation of an SMM may emerge.[5] Experimentally, an SMM shows superparamagnet-like properties, exhibiting both frequency-dependent out-of-phase alternating-current (ac) magnetic susceptibility signals and hysteresis loops, the diagnostic property of a magnet.

In their vast majority, structurally impressive metal carboxylate clusters and SMMs have been prepared to date either through the exclusive use of RCO_2^- ions in hydrolysis/alcoholysis reactions[1] or via self-assembly reactions of metal carboxylate precursors and various multidentate chelating/bridging organic ligands, such as pyridyl alcohols, polyols (i.e., diols and triols), oximes, and Schiff bases.[6] Although simple and flexible carboxylates (i.e., $MeCO_2^-$, Bu^tCO_2H), as well as sterically demanding and robust ones (i.e., aromatic RCO_2^-), have been widely and successfully used in 3d/4f-metal cluster chemistry,[4,5] the *tert*-butylacetate ion ($Bu^tCH_2CO_2^-$) has not

Received: May 25, 2015
Published: July 22, 2015

DOI: 10.1021/acs.inorgchem.5b01179
Inorg. Chem. 2015, 54, 7555−7561

yet attracted similar attention. Reasons that differentiate the $Bu^tCH_2CO_2^-$ group from the structurally analogous pivalate ion ($Bu^tCO_2^-$) are mainly steric and partially electronic. For instance, *tert*-butylacetate ion is larger in size, but more flexible (i.e., free rotation around the $C_{Bu}-CH_2$ single bond), than the pivalate ion. Further, although $Bu^tCH_2CO_2H$ and Bu^tCO_2H have similar pk_a values (close to 5.0), the acidity of the former is higher than that of the latter due to solvation effects.[7]

Given the absence of any previous use of the $Bu^tCH_2CO_2^-$ group in 3d/4f-metal cluster chemistry, we started a program aiming at the systematic investigation of possible structural alterations induced by the presence of *tert*-butylacetate ions in systems that were known to include coordinated pivalate or other carboxylate ions. To that end, we decided to study the $Cu^{II}/Gd^{III}/Bu^tCH_2CO_2^-/pdmH_2$ reaction system, where $pdmH_2$ is the tridentate (N,O,O) ligand pyridine-2,6-dimethanol (Scheme 1). This system has previously yielded

Scheme 1. Structural Formula and Abbreviation of the Ligand Pyridine-2,6-dimethanol ($pdmH_2$) Used in This Study

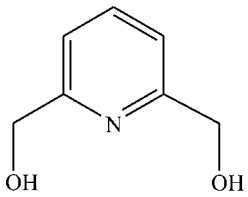

$pdmH_2$

structurally novel and magnetically interesting $\{Cu_3Gd_6\}$[8a] and $\{Cu_{15}Gd_7\}$[8b] clusters with pivalates and benzoates, respectively, under similar reaction conditions. However, the reaction of $[Cu_2(O_2CCH_2Bu^t)_4(HO_2CCH_2Bu^t)_2]$, $Gd(NO_3)_3\cdot 6H_2O$, $pdmH_2$, and NEt_3 in a 1:2:2:4 molar ratio in MeCN/MeOH gave instead blue crystals of the new compound $[Cu_4Gd_8(OH)_6(NO_3)_2(O_2CCH_2Bu^t)_{16}(pdm)_4]$ (**1**). Complex **1** is the first 3d/4f-metal cluster obtained from the use of *tert*-butylacetate ions, and together with the isostructural $\{Cu_4Tb_8\}$ (**2**), $\{Cu_4Dy_8\}$ (**3**), and $\{Cu_4La_8\}$ (**4**) analogues are the first complexes with a $\{Cu_4Ln_8\}$ stoichiometry, which is also unprecedented for all transition metals. Herein, we report the preparation, characterization, and study of **1**−**4**.

EXPERIMENTAL SECTION

Syntheses. All manipulations were performed under aerobic conditions using materials (reagent grade) and solvents as received. $[Cu_2(O_2CCH_2Bu^t)_4(HO_2CCH_2Bu^t)_2]$ was prepared as a blue-green microcrystalline solid in high yield (~90%) by the reaction of freshly prepared $CuCO_3$ and an excess of $Bu^tCH_2CO_2H$ in a solvent mixture comprising H_2O and Me_2CO (1:1 molar ratio). Anal. Calcd (Found) for the vacuum-dried $[Cu_2(O_2CCH_2Bu^t)_4(HO_2CCH_2Bu^t)_2]$: C 52.73 (52.66), H 8.36 (8.22).

*$[Cu_4Gd_8(OH)_6(NO_3)_2(O_2CCH_2Bu^t)_{16}(pdm)_4]$ (**1**).* To a stirred, pale yellow solution of $pdmH_2$ (0.03 g, 0.2 mmol) and NEt_3 (0.056 mL, 0.4 mmol) in MeCN/MeOH (20 mL, 3:1 v/v) were added solids $Gd(NO_3)_2\cdot 6H_2O$ (0.09 g, 0.2 mmol) and $[Cu_2(O_2CCH_2Bu^t)_4(HO_2CCH_2Bu^t)_2]$ (0.08 g, 0.1 mmol) at the same time. The resulting, blue-colored suspension was stirred for a further 30 min and filtered, and the filtrate was allowed to slowly evaporate at room temperature. After 20 days, X-ray quality blue crystals of $\mathbf{1}\cdot 3.4MeCN\cdot 0.4MeOH\cdot 0.7H_2O$ were collected by filtration, washed with cold MeCN (2 × 3 mL) and Et_2O (2 × 3 mL), and dried under vacuum; the yield was 40%. The crystalline solid was analyzed as solvent-free **1**. Anal. Calcd: C, 36.07; H, 5.13; N, 2.04%. Found: C, 36.41; H, 5.37; N, 2.35%. Selected IR data (KBr, cm^{-1}) for **1**: 3256 (s), 2952 (s), 1564 (m), 1436 (m), 1412 (m), 1384 (m), 1300 (w), 1236 (m), 1196 (m), 1058 (m), 778 (m), 742 (m), 640 (m), 500 (m).

*$[Cu_4Tb_8(OH)_6(NO_3)_2(O_2CCH_2Bu^t)_{16}(pdm)_4]$ (**2**), $[Cu_4Dy_8(OH)_6(NO_3)_2(O_2CCH_2Bu^t)_{16}(pdm)_4]$ (**3**), and $[Cu_4La_8(OH)_6(NO_3)_2(O_2CCH_2Bu^t)_{16}(pdm)_4]$ (**4**).* All complexes (**2**−**4**) were prepared in the same manner as complex **1** but using $Tb(NO_3)_3\cdot 5H_2O$ (0.09 g, 0.2 mmol), $Dy(NO_3)_3\cdot 5H_2O$ (0.09 g, 0.2 mmol), and $La(NO_3)_3\cdot 6H_2O$ (0.09 g, 0.2 mmol) as the lanthanide salt. Single crystals of sufficient size to allow for single-crystal X-ray crystallographic studies were not grown under multiple different crystallization techniques and conditions. However, all the obtained bluish microcrystalline products of complexes **2**−**4** were collected by filtration, washed with cold MeCN (2 × 3 mL) and Et_2O (2 × 3 mL), and dried under vacuum; the yields were 30% (**2**), 32% (**3**), and 43% (**4**). We have confirmed the identities of **2**−**4** by (i) IR spectroscopic comparison with the authentic, single-crystalline sample of **1** (Figure S1), and (ii) elemental analyses. Elemental analysis (%) calcd for lattice solvent-free **2**: C, 35.95; H, 5.11; N, 2.03%. Found: C, 36.23; H, 5.02; N, 2.13%. Elemental analysis (%) calcd for lattice solvent-free **3**: C, 35.71; H, 5.07; N, 2.01%. Found: C, 35.87; H, 5.18; N, 1.94%. Elemental analysis (%) calcd for lattice solvent-free **4**: C, 37.40; H, 5.32; N, 2.11%. Found: C, 37.55; H, 5.46; N, 2.07%.

X-ray Crystallography. A blue single-crystal of complex $\mathbf{1}\cdot 3.4MeCN\cdot 0.4MeOH\cdot 0.7H_2O$ (0.18 × 0.11 × 0.11 mm) was taken from the mother liquor and immediately cooled at 170(2) K. Diffraction measurements were made on a Rigaku R-AXIS SPIDER Image Plate diffractometer using graphite-monochromated Cu Kα radiation. Data collection (ω-scans) and processing (cell refinement, data reduction, and empirical absorption correction) were performed using the CrystalClear program package.[9] The structure was solved by direct methods using SHELXS-97 and refined by full-matrix least-squares techniques on F^2 with SHELXL-97.[10] All H atoms either were located by difference maps and refined isotropically or were introduced at calculated positions as riding on their respective atoms. All non-H atoms were refined anisotropically. Important crystallographic data are listed in Table 1. Further crystallographic details can be found in the corresponding CIF file provided in the Supporting Information. Crystallographic data (excluding structure factors) for the structure reported in this work have been deposited to the Cambridge Crystallographic Data Centre (CCDC); deposition number: CCDC-1046297.

Physical Measurements. Infrared (IR) spectra were recorded in the solid state (KBr pellet) on a PerkinElmer 16 PC FT spectrometer in the 4000−400 cm^{-1} range. Elemental analyses (C, H, and N) were performed by the University of Patras microanalysis service. Direct current (dc) and alternating current (ac) magnetic susceptibility studies were performed at the University of Barcelona Chemistry Department on a DSM5 Quantum Design magnetometer operating at 0.3 T in the 300−30 K range and at 0.02 T in the 30−2.0 K range to avoid saturation effects. Pascal's constants were used to estimate the diamagnetic correction, which was subtracted from the experimental susceptibility to give the molar paramagnetic susceptibility (χ_M).[11]

RESULTS AND DISCUSSION

Synthetic Comments. The organic chelating/bridging ligand pyridine-2,6-dimethanol ($pdmH_2$) is a well-explored group in transition-metal[12] and lanthanide[13] cluster chemistry, yielding structurally novel and magnetically interesting compounds. In contrast, its previous use in 3d/4f-metal cluster chemistry had been very limited,[14] until our[8b] and Brechin's[8a] groups initiated the systematic investigation of the $Cu^{II}/Ln^{III}/RCO_2^-/pdmH_2$ reaction system, where Ln are various lanthanides and R can include various substituents, such as Me-, Bu^t-, Ph-, among others. From very similar reactions between Cu^{II} and Gd^{III} sources, $pdmH_2$, NEt_3, and RCO_2^-

DOI: 10.1021/acs.inorgchem.5b01179
Inorg. Chem. 2015, 54, 7555−7561

Table 1. Crystallographic Data for Complex 1

	$C_{131.2}H_{223.2}Cu_4Gd_8N_{9.4}O_{53.1}$
fw (g mol^{-1})	4294.15
crystal system	triclinic
space group	$P\bar{1}$
a (Å)	16.1708(3)
b (Å)	17.2594(3)
c (Å)	18.8906(3)
α (deg)	93.324(1)
β (deg)	113.445(1)
γ (deg)	99.843(1)
V (Å^3)	4719.3(1)
Z	1
T (K)	170(2)
radiation	Cu Kα
ρ_{calcd} (g cm^{-3})	1.511
μ (mm^{-1})	18.892
$2\theta_{max}$ (deg)	125
reflns collected/unique/used	71127/14336 (R_{int} = 0.0881)/14336
parameters refined	929
reflections [$I > 2\sigma(I)$]	10524
R_1[a]	0.0647
wR_2[a]	0.1565
$(\Delta\rho)_{max,min}$ (e Å^{-3})	1.517/−1.733

[a] $w = 1/[\sigma^2(F_o^2) + (\alpha P)^2 + bP]$ and $P = [\max(F_o^2,0) + 2F_c^2]/3$, $R_1 = \sum(|F_o| - |F_c|)/\sum(|F_o|)$, and $wR_2 = \{\sum[w(F_o^2 - F_c^2)^2]/\sum[w(F_o^2)^2]\}^{1/2}$.

ions, two different complexes have been isolated and structurally characterized, clearly emphasizing the effect of the carboxylate ion on the chemical identity of the heterometallic cluster compounds. When R = Bu^t-, the nonanuclear $[Cu_3Gd_6(OH)(CO_3)_4(O_2CBu^t)_9(pdm)_3(MeOH)_3]$ complex was obtained,[8a] whereas, for R = Ph, the $[Cu_{15}Gd_7(OH)_6(CO_3)_4(O_2CPh)_{19}(pdm)_9(pdmH_2)_3(H_2O)_2]$ cage-like cluster was resulted in good yields.[8b]

In an attempt to further investigate the above-mentioned reaction system, we decided to use a nonpreviously employed in 3d/4f-cluster chemistry carboxylate ion (i.e., $Bu^tCH_2CO_2^-$) without altering any of the other important synthetic variables (i.e., reactions solvents, crystallization method, temperature, etc.). Thus, from the reaction between $[Cu_2(O_2CCH_2Bu^t)_4(HO_2CCH_2Bu^t)_2]$ starting material, $Gd(NO_3)_3{\cdot}6H_2O$, $pdmH_2$, and NEt_3 in a 1:2:2:4 molar ratio in MeCN/MeOH, we have been able to isolate blue crystals of a new $[Cu_4Gd_8(OH)_6(NO_3)_2(O_2CCH_2Bu^t)_{16}(pdm)_4]$ (**1**) compound in 40% yield. The analogous reactions with the corresponding lanthanide nitrate salts led to the isostructural $[Cu_4Tb_8(OH)_6(NO_3)_2(O_2CCH_2Bu^t)_{16}(pdm)_4]$ (**2**), $[Cu_4Dy_8(OH)_6(NO_3)_2(O_2CCH_2Bu^t)_{16}(pdm)_4]$ (**3**), and $[Cu_4La_8(OH)_6(NO_3)_2(O_2CCH_2Bu^t)_{16}(pdm)_4]$ (**4**) complexes in similar to **1** overall yields. The general formation of **1**−**4** is summarized in stoichiometric eq 1. Complexes **1**−**4** are very stable under the prevailing basic conditions, and their identities are not affected by either the nature of the base or the molar ratio of the reagents. However, their crystallinity is heavily affected by the appropriate solvent mixture (MeCN/MeOH); the same reactions in pure MeCN or MeOH gave microcrystalline solids which were identified as $\{Cu_4Ln_8\}$ from IR spectroscopic studies and elemental analyses. As expected from the presence of nitrato ligands in the structure of **1** (*vide infra*), the analogous reactions with $Gd(ClO_4)_3$ or $GdCl_3$ starting materials have not afforded **1**, but greenish precipitates of new products which we have not been able to crystallize and eventually determine their crystal structures.

$$4Cu^{2+} + 8Ln^{3} + 16Bu^tCH_2CO_2^- + 2NO_3^- + 4pdmH_2 + 6H_2O + 14NEt_3 \xrightarrow[MeOH]{MeCN} [Cu_4Ln_8(OH)_6(NO_3)_2(O_2CCH_2Bu^t)_{16}(pdm)_4] + 14NHEt_3^+ \quad Ln = Gd\ (\mathbf{1});\ Tb\ (\mathbf{2});\ Dy\ (\mathbf{3});\ La\ (\mathbf{4}) \qquad (1)$$

Description of Structure. Representative complex **1**·3.4MeCN·0.4MeOH·0.7H_2O was characterized by single-crystal X-ray crystallography, while the identities of the analogues **2**−**4** were established by elemental analyses (C, H, N), and IR spectral comparison with crystals of **1** (Figure S1). The formula of **1** is based on metric parameters (Table 2), charge-balance considerations, and bond-valence-sum (BVS) calculations[15] on the O atoms (Table 3). The lattice solvate molecules will not be further discussed.

Table 2. Selected Interatomic Distances (Angstroms) and Angles (deg) for Complex 1[a]

Cu1−O1	1.947(6)	Cu2−O3	2.345(6)
Cu1−O2	1.961(6)	Cu2−O10	1.947(6)
Cu1−O6	2.746(7)	Cu2−O12	1.949(7)
Cu1−O25′	1.905(6)	Cu2−O22	1.913(6)
Cu1−N1	1.899(8)	Cu2−O23	1.982(5)
Gd1−O2	2.269(6)	Gd3−O7	2.396(6)
Gd1−O3	2.363(6)	Gd3−O13	2.476(5)
Gd1−O6	2.418(6)	Gd3−O14	2.536(6)
Gd1−O8	2.424(7)	Gd3−O19	2.393(6)
Gd1−O9	2.382(6)	Gd3−O21	2.429(5)
Gd1−O21	2.342(5)	Gd3−O22	2.409(5)
Gd1−O22	2.399(5)	Gd3−O23	2.412(6)
Gd1−O25′	2.805(5)	Gd3−O24	2.434(5)
Gd2−O3	2.309(5)	Gd3−O26	2.504(5)
Gd2−O4	2.479(6)	Gd4−O1′	2.344(6)
Gd2−O5′	2.334(5)	Gd4−O13	2.396(6)
Gd2−O11	2.368(6)	Gd4−O15	2.451(7)
Gd2−O21	2.367(6)	Gd4−O16	2.456(7)
Gd2−O23	2.444(6)	Gd4−O17	2.433(7)
Gd2−O26′	2.408(5)	Gd4−O18	2.415(6)
Gd2−N2	2.525(8)	Gd4−O20	2.346(7)
		Gd4−O24	2.374(5)
Cu1−O1−Gd4′	128.7(3)	Gd1−O3−Gd2	108.7(2)
Cu1−O2−Gd1	106.4(2)	Gd1−O21−Gd2	107.5(2)
Cu1−O25′-Gd1	90.1(2)	Gd1−O21−Gd3	104.8(2)
Cu1−O6−Gd1	81.9(2)	Gd1−O22−Gd3	103.7(2)
Cu2−O3−Gd1	92.2(2)	Gd2−O21−Gd3	112.0(2)
Cu2−O3−Gd2	89.8(2)	Gd2−O23−Gd3	109.9(2)
Cu2−O22−Gd1	103.1(3)	Gd3−O13−Gd4	106.6(2)
Cu2−O22−Gd3	106.4(2)	Gd3−O24−Gd4	108.7(2)
Cu2−O23−Gd2	95.3(2)	Gd3−O26−Gd2′	138.0(2)
Cu2−O23−Gd3	104.0(2)		

[a] Symmetry code: ′ = 1 − x, −y, −z.

The centrosymmetric molecular structure of **1** consists of a $\{Cu^{II}_4Gd^{III}_8\}$ cage-like cluster (Figure 1, top) with an unusual topology built from two $\{CuGd_3\}$ cubanes which are linked to each other and to two $\{CuGd\}$ subunits on opposite sides through two $\eta^2{:}\eta^2{:}\eta^2{:}\mu_5$ NO_3^- ions (Figure 1, bottom). The metal ions within each cubane are bridged by three μ_3-OH^- (O21, O22, O23) and a μ_3-OR^- (O3) group from the alkoxido arm of an $\eta^1{:}\eta^1{:}\eta^3{:}\mu_3$ pdm^{2-} ligand. In addition to the bridging

DOI: 10.1021/acs.inorgchem.5b01179
Inorg. Chem. 2015, 54, 7555−7561

Table 3. Bond Valence Sum (BVS) Calculations for Selected Oxygen Atoms in 1[a]

	BVS	assignment
O21	1.17	OH^-
O22	1.22	OH^-
O23	1.10	OH^-

[a]A BVS in the ∼1.8−2.0, ∼1.0−1.3, and ∼0.2−0.4 ranges for an O atom is indicative of non-, single-, and double-protonation, respectively, but can be altered somewhat by hydrogen bonding.

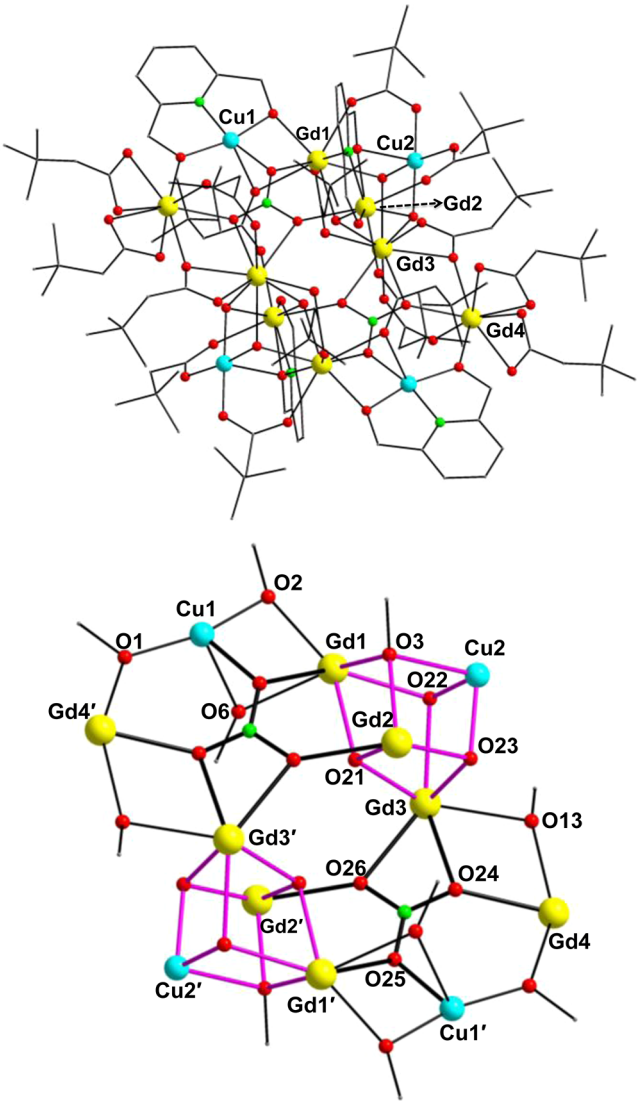

Figure 1. (top) The structure of **1** and (bottom) its complete $[Cu_4Gd_8(\mu_5\text{-}NO_3)_2(\mu_3\text{-}OH)_6(\mu_3\text{-}OR)_2(\mu\text{-}OR)_8]^{14+}$ core, highlighting with black and purple thick bonds the μ_5-NO_3^- groups and the cubane subunits, respectively. H atoms are omitted for clarity. Color scheme: Cu^{II} cyan, Gd^{III} yellow, O red, N green, C gray. Primes are used for symmetry-related atoms; see the footnote of Table 2.

nitrato groups, eight in total μ-OR^- bridges from two $\eta^2{:}\eta^1{:}\eta^2{:}\mu_3$ pdm^{2-} and four $\eta^1{:}\eta^2{:}\mu$ and $\eta^1{:}\eta^2{:}\mu_3$ $Bu^tCH_2CO_2^-$ ligands serve to link the extrinsic {CuGd} subunits with the cubane metal ions. The complete core is thus $[Cu_4Gd_8(\mu_5\text{-}NO_3)_2(\mu_3\text{-}OH)_6(\mu_3\text{-}OR)_2(\mu\text{-}OR)_8]^{14+}$ (Figure 1, bottom). Peripheral ligation about the core is provided by the N,O,O-chelating part of the pdm^{2-} groups and, more impressively, by the oxygen atoms of 16 bridging $Bu^tCH_2CO_2^-$ ligands; the latter are arranged into five classes, adopting a total of six different binding modes with the metal centers (Figure 2). This

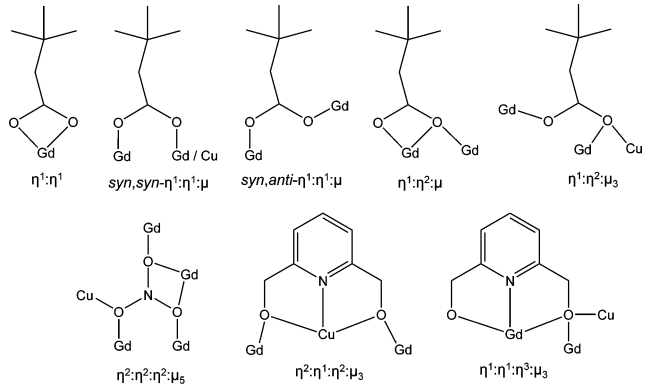

Figure 2. Crystallographically established coordination modes of $Bu^tCH_2CO_2^-$, NO_3^-, and pdm^{2-} ligands present in complex **1**.

illustrates the flexibility, versatility, and coordinating ability of *tert*-butylacetate ions, presumably deriving from the combination of its basic character and rotational freedom about the $C_{Bu}-CH_2$ single bond.

All Cu ions are five-coordinate with almost ideal square pyramidal geometries (τ = 0.04 and 0.01 for Cu1 and Cu2, respectively[16a]). All Gd ions are eight-coordinate, except from Gd3 and Gd3′, which are 9-coordinate. The program SHAPE[16b] was used to estimate the closer coordination polyhedra defined by the donor atoms around all Gd atoms in **1**. The best fit was obtained for the triangular dodecahedral (Gd1, Gd2, Gd4) and muffin (Gd3) geometries (Figure 3),

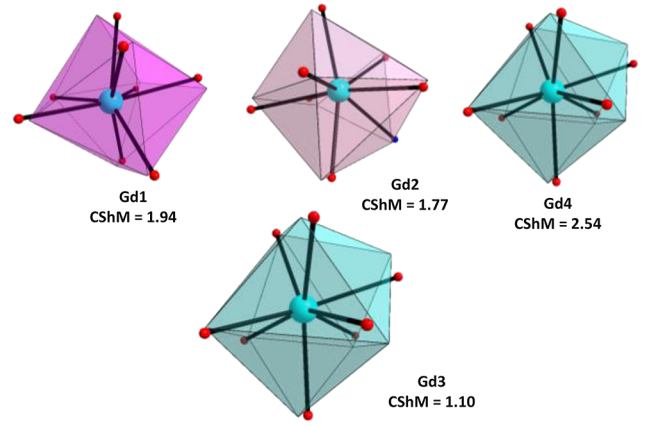

Figure 3. Triangular dodecahedron coordination spheres of Gd1, Gd2, and Gd4 (top) and muffin geometry of Gd3 (bottom) in the structure of **1**. Points connected by the black thin lines define the vertices of the ideal polyhedron.

with CShM values of 1.94, 1.77, 2.54, and 1.10, respectively. Values of CShM between 0.1 and 3 usually correspond to a not negligible, but still small, distortion from ideal geometry. Finally, there are no significant intermolecular interactions in the crystal structure of **1**, only weak contacts between the solvate molecules and the peripheral ligands. The shortest intermolecular metal···metal distance is 11 Å, between the Gd1 atoms in neighboring molecules.

DOI: 10.1021/acs.inorgchem.5b01179
Inorg. Chem. 2015, 54, 7555−7561

Solid-State Magnetic Susceptibility Studies. Solid-state direct-current (dc) magnetic susceptibility (χ_M) data on dried and analytically pure samples of **1**−**4** were collected in the 2.0−300 K range and are plotted as $\chi_M T$ vs T in Figure 4. The

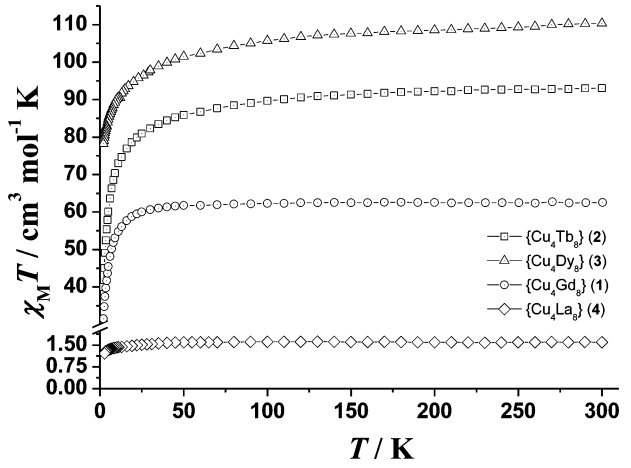

Figure 4. $\chi_M T$ vs T plots for **1**−**4**. Lines are guides to the eye.

magnetic response of the {Cu_4La_8} (**4**) complex (La^{III} is diamagnetic) agrees with four magnetically isolated Cu^{II} ions, as expected from the structural features of **1** (i.e., isolated Cu^{II} ions), and confirms the presence of four noninteracting Cu^{II} ions. The $\chi_M T$ product of **4** remains essentially constant at a value of 1.60 cm^3 K mol^{-1} from 300 to 2 K, very close to the theoretical 1.65 cm^3 K mol^{-1} for four noninteracting Cu^{II} ions (g = 2.1). For clusters **1**−**3**, the experimental $\chi_M T$ values at 300 K are all in excellent agreement with the theoretical ones (64.65 cm^3 K mol^{-1} for **1**; 96.21 cm^3 K mol^{-1} for **2**; 115.01 cm^3 K mol^{-1} for **3**) for 4 Cu^{II} and 8 Ln^{III} noninteracting ions. In all complexes, the $\chi_M T$ products remain almost constant at values of ∼62.6 (**1**), 93.1 (**2**), and 110.4 (**3**) cm^3 K mol^{-1} from 300 K to ∼50 K, and then steadily decrease to minimum values of 31.53 (**1**), 39.97 (**2**), and 78.86 (**3**) cm^3 K mol^{-1} at 2.0 K, indicating the presence of predominant antiferromagnetic exchange interactions between the metal centers and/or depopulation of the excited M_J states when the 4f-metal ion is Tb^{III} or Dy^{III}.[3,5] Due to the many different magnetic exchange pathways involved into the superexchange mechanism, it is not possible to accurately propose a ground-state spin value for **1** based on a simplistic "spin-up" vs "spin-down" vector scheme. Undoubtedly, the shape of the $\chi_M T$ vs T plot for **1** indicates the presence of predominant antiferromagnetic exchange interactions which most likely result from the $Cu^{2+}\cdots Gd^{3+}$ and/or $Gd^{3+}\cdots Gd^{3+}$ interactions within the {$CuGd_3$} cubanes, the {CuGd} subunits, and/or between the two different fragments.

Magnetization (M) vs field (H) studies for **1** at 2 K (Figure 5) show a continuous increase of M as H increases, indicating the presence of weak antiferromagnetic interactions and low-lying excited states. The magnetization of **1** reaches a maximum value of 55.2 $N\mu_B$ at 5 T, very close to the maximum value of 60 $N\mu_B$ expected for 4 Cu^{II} and 8 Gd^{III} coupled ions. The field dependence of the magnetization of **1** is below the Brillouin function for the sum of isolated metal ions, thus confirming the weak antiferromagnetic exchange interactions. The magnetization measurements for the anisotropic {Cu_4Tb_8} and {Cu_4Dy_8} analogues (Figure S2) show a similar trend to that of **1**, with the lack of true saturation in magnetization mainly

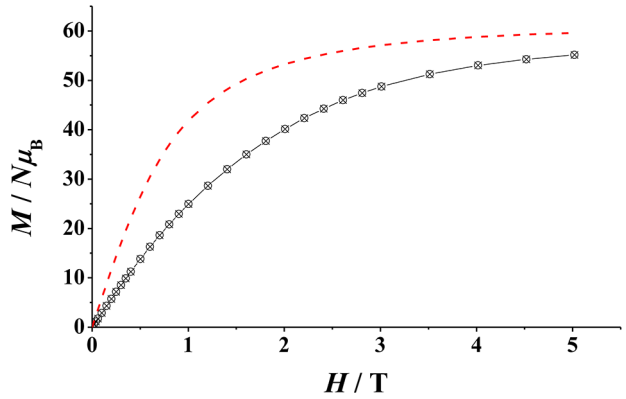

Figure 5. M vs H plot of complex **1** at 2 K. The Brillouin function for four Cu^{II} and eight Gd^{III} ions is shown by the dashed red line. Solid line is a guide for the eye.

attributed to the presence of magnetic anisotropy, population of low-lying excited states, and weak antiferromagnetic interactions between the metal centers.[5]

ac magnetic susceptibility studies have been also carried out in order to investigate the magnetization dynamics of the anisotropic **2** and **3** analogues in the absence of a dc magnetic field. Complex **3** shows frequency-dependent out-of-phase χ''_M tails of signals at temperatures below ∼5 K (Figure 6, top),

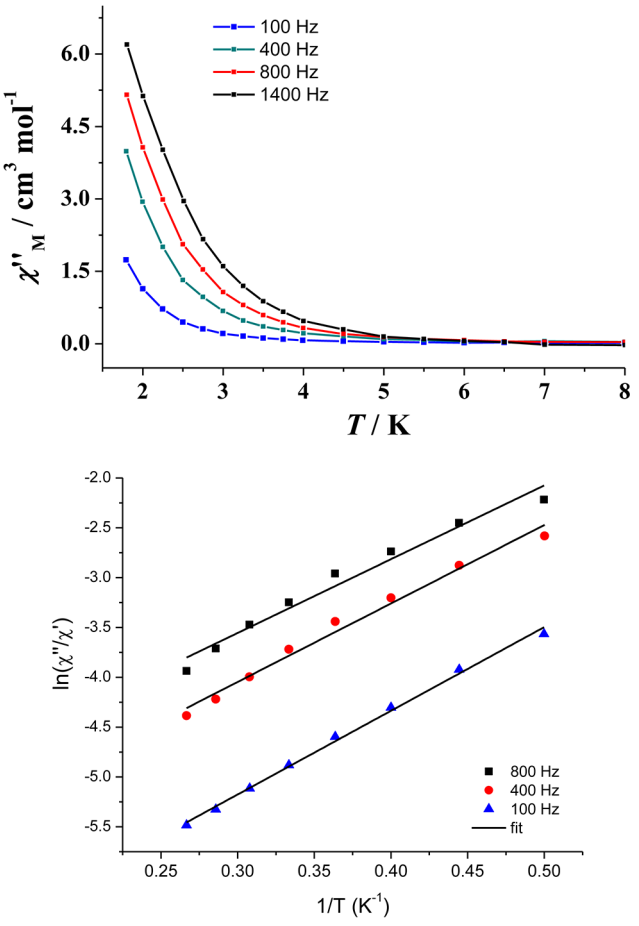

Figure 6. (top) Out-of-phase (χ''_M) vs T ac susceptibility signals for **3** in a 4 G field oscillating at the indicated frequencies. (bottom) Plots of ln(χ''/χ') vs 1/T for **3** at different ac frequencies; the solid lines are the best-fit curves.

DOI: 10.1021/acs.inorgchem.5b01179
Inorg. Chem. 2015, 54, 7555−7561

characteristic of the slow magnetization relaxation of an SMM with a small energy barrier for the magnetization reversal. Such behavior is most likely attributed to single-ion effects of the individual Dy^{III} Kramer ions[3] within **3**. Attempts to suppress the fast tunneling, responsible for the lack of entirely visible out-of-phase peaks, through the use of a dc field all failed to yield any noticeable shift of the χ''_M signals to higher T. Complex **2** did not show any χ''_M signals in either the absence or the presence of an external dc field. Given the lack of χ'' peak maxima, the energy barrier and relaxation time for **3** were approximated using a method employed by Bartolomé et al.,[17] based on the equation: $\ln(\chi''/\chi') = \ln(\omega\tau_0) + E_a/k_BT$. Considering a single relaxation process, the least-squares fits of the experimental data (Figure 6, bottom) gave an average energy barrier of ~5.5(3) cm^{-1} (~7.9(3) K) and a relaxation time of $4.9(4) \times 10^{-7}$ s, consistent with the expected τ_0 values for a fast-relaxing SMM.

CONCLUSIONS

In conclusion, we have shown that it is indeed possible to synthesize new cluster compounds with aesthetically pleasing structures and interesting magnetic properties by utilizing an unexplored in 3d/4f-metal cluster chemistry carboxylate group. Reaction systems already saturated with "old" results can be now reconsidered and re-explored in the presence of *tert*-butylacetate ions. Ongoing studies reveal increasingly new $Bu^tCH_2CO_2^-$-based products with unforeseen structures and properties, clearly presaging a new area of research in 3d-, 4f-, and 3d/4f-metal cluster chemistry.

ASSOCIATED CONTENT

Supporting Information

Crystallographic data (CIF format), and various spectroscopic and magnetism figures. The Supporting Information is available free of charge on the ACS Publications website at DOI: 10.1021/acs.inorgchem.5b01179.

AUTHOR INFORMATION

Corresponding Authors

*E-mail: perlepes@upatras.gr (S.P.P.).
*E-mail: tstamatatos@brocku.ca (Th.C.S.).

Notes

The authors declare no competing financial interest.

ACKNOWLEDGMENTS

This work was supported by the CICYT (project CTQ2012-30662, to A.E.), the ARISTEIA Action (Project code 84, acronym MAGCLOPT) of the Operational Programme "Education and Lifelong Learning", cofunded by ESF and National Resources (to S.P.P.), and the NSERC Discovery Grant (to Th.C.S.).

REFERENCES

(1) (a) Tasiopoulos, A. J.; Vinslava, A.; Wernsdorfer, W.; Abboud, K. A.; Christou, G. *Angew. Chem., Int. Ed.* **2004**, *43*, 2117−2121. (b) Whitehead, G. F. S.; Moro, F.; Timco, G. A.; Wernsdorfer, W.; Teat, S. J.; Winpenny, R. E. P. *Angew. Chem.* **2013**, *125*, 10116−10119. (c) Soler, M.; Wernsdorfer, W.; Folting, K.; Pink, M.; Christou, G. *J. Am. Chem. Soc.* **2004**, *126*, 2156−2165. (d) Peng, J.-B.; Zhang, Q.-C.; Kong, X.-J.; Ren, Y.-P.; Long, L.-S.; Huang, R.-B.; Zheng, L.-S.; Zheng, Z. *Angew. Chem., Int. Ed.* **2011**, *50*, 10649−10652.

(2) Alexandropoulos, D. I.; Mowson, A. M.; Pilkington, M.; Bekiari, V.; Christou, G.; Stamatatos, Th. C. *Dalton Trans.* **2014**, *43*, 1965−1969.

(3) (a) Woodruff, D. N.; Winpenny, R. E. P.; Layfield, R. A. *Chem. Rev.* **2013**, *113*, 5110−5148. (b) Rinehart, J. D.; Long, J. R. *Chem. Sci.* **2011**, *2*, 2078−2085. (c) Zhang, P.; Zhang, L.; Tang, J. *Dalton Trans.* **2015**, *44*, 3923−3929. (d) Zhang, P.; Zhang, L.; Wang, C.; Xue, S.; Lin, S.-Y.; Tang, J. *J. Am. Chem. Soc.* **2014**, *136*, 4484−4487. (e) Ungur, L.; Lin, S.-Y.; Tang, J.; Chibotaru, L. F. *Chem. Soc. Rev.* **2014**, *43*, 6894−6905.

(4) (a) Andruh, M.; Ramade, I.; Codjovi, E.; Guillou, O.; Kahn, O.; Trombe, J. C. *J. Am. Chem. Soc.* **1993**, *115*, 1822−1829. (b) Zheng, Y.-Z.; Zhou, G.-J.; Zheng, Z.; Winpenny, R. E. P. *Chem. Soc. Rev.* **2014**, *43*, 1462−1475.

(5) (a) Aronica, C.; Pilet, G.; Chastanet, G.; Wernsdorfer, W.; Jacquot, J.-F.; Luneau, D. *Angew. Chem., Int. Ed.* **2006**, *45*, 4659−4662. (b) Langley, S. K.; Ungur, L.; Chilton, N. F.; Moubaraki, B.; Chibotaru, L. F.; Murray, K. S. *Chem. - Eur. J.* **2011**, *17*, 9209−9218. (c) Baskar, V.; Gopal, K.; Helliwell, M.; Tuna, F.; Wernsdorfer, W.; Winpenny, R. E. P. *Dalton Trans.* **2010**, *39*, 4747−4750.

(6) For example, see: (a) Moushi, E. E.; Lampropoulos, C.; Wernsdorfer, W.; Nastopoulos, V.; Christou, G.; Tasiopoulos, A. J. *J. Am. Chem. Soc.* **2010**, *132*, 16146−16155. (b) Athanasopoulou, A. A.; Pilkington, M.; Raptopoulou, C. P.; Escuer, A.; Stamatatos, Th. C. *Chem. Commun.* **2014**, *50*, 14942−14945. (c) Brechin, E. K. *Chem. Commun.* **2005**, 5141−5153. (d) Tasiopoulos, A. J.; Perlepes, S. P. *Dalton Trans.* **2008**, 5537−5555.

(7) Cox, B. G. *Acids and Bases: Solvent Effects on Acid-Base Strength*; Oxford University Press: Oxford, U.K., 2013.

(8) (a) Hooper, T. N.; Inglis, R.; Palacios, M. A.; Nichol, G. S.; Pitak, M. B.; Coles, S. J.; Lorusso, G.; Evangelisti, M.; Brechin, E. K. *Chem. Commun.* **2014**, *50*, 3498−3500. (b) Dermitzaki, D.; Lorusso, G.; Raptopoulou, C. P.; Psycharis, V.; Escuer, A.; Evangelisti, M.; Perlepes, S. P.; Stamatatos, Th. C. *Inorg. Chem.* **2013**, *52*, 10235−10237.

(9) *CrystalClear*; Rigaku/MSC Inc.: The Woodlands, Texas, 2005.

(10) (a) Sheldrick, G. M. *SHELXS-97: Program for Crystal Structure Solution*; University of Göttingen: Göttingen, Germany, 1997. (b) Sheldrick, G. M. *Acta Crystallogr., Sect. A: Found. Crystallogr.* **2008**, *64*, 112−122. (c) Sheldrick, G. M. *SHELXL-97: Program for Crystal Structure Refinement*; University of Göttingen: Göttingen, Germany, 1997.

(11) Bain, G. A.; Berry, J. F. *J. Chem. Educ.* **2008**, *85*, 532−536.

(12) For some representative examples, see: (a) Stamatatos, Th. C.; Vlahopoulou, G. C.; Raptopoulou, C. P.; Terzis, A.; Escuer, A.; Perlepes, S. P. *Inorg. Chem.* **2009**, *48*, 4610−4612. (b) Taguchi, T.; Stamatatos, Th. C.; Abboud, K. A.; Jones, C. M.; Poole, K. M.; O' Brien, T. A.; Christou, G. *Inorg. Chem.* **2008**, *47*, 4095−4108. (c) Taguchi, T.; Thompson, M. S.; Abboud, K. A.; Christou, G. *Dalton Trans.* **2010**, *39*, 2131−2133. (d) Murugesu, M.; Habrych, M.; Wernsdorfer, W.; Abboud, K. A.; Christou, G. *J. Am. Chem. Soc.* **2004**, *126*, 4766−4767. (e) Stamatatos, Th. C.; Abboud, K. A.; Wernsdorfer, W.; Christou, G. *Angew. Chem., Int. Ed.* **2007**, *46*, 884−888. (f) Alexopoulou, K. I.; Raptopoulou, C. P.; Psycharis, V.; Terzis, A.; Tangoulis, V.; Stamatatos, Th. C.; Perlepes, S. P. *Aust. J. Chem.* **2012**, *65*, 1608−1619. (g) Stamatatos, Th. C.; Poole, K. M.; Abboud, K. A.; Wernsdorfer, K. A.; O' Brien, T. A.; Christou, G. *Inorg. Chem.* **2008**, *47*, 5006−5021. (h) Vlahopoulou, G. C.; Alexandropoulos, D. I.; Raptopoulou, C. P.; Perlepes, S. P.; Escuer, A.; Stamatatos, Th. C. *Polyhedron* **2009**, *28*, 3235−3242. (i) Katsoulakou, E.; Dermitzaki, D.; Konidaris, K. F.; Moushi, E. E.; Raptopoulou, C. P.; Psycharis, V.; Tasiopoulos, A. J.; Bekiari, V.; Manessi-Zoupa, E.; Perlepes, S. P.; Stamatatos, Th. C. *Polyhedron* **2013**, *52*, 467−475.

(13) (a) Yang, P.-P.; Gao, X.-F.; Song, H.-B.; Zhang, S.; Mei, X.-L.; Li, L.-C.; Liao, D.-Z. *Inorg. Chem.* **2011**, *50*, 720−722. (b) Yang, P.-P. *Z. Anorg. Allg. Chem.* **2011**, *637*, 1234−1237. (c) Alexandropoulos, D. I.; Cunha-Silva, L.; Pham, L.; Bekiari, V.; Christou, G.; Stamatatos, Th. C. *Inorg. Chem.* **2014**, *53*, 3220−3229.

(14) (a) Murugesu, M.; Mishra, A.; Abboud, K. A.; Christou, G.; Wernsdorfer, W. *Polyhedron* **2006**, *25*, 613−625. (b) Zhao, X.-Q.; Lan,

DOI: 10.1021/acs.inorgchem.5b01179
Inorg. Chem. 2015, 54, 7555−7561

Y.; Zhao, B.; Cheng, P.; Anson, C. E.; Powell, A. K. *Dalton Trans.* **2010**, *39*, 4911−4917.
(15) Brown, I. D.; Altermatt, D. *Acta Crystallogr., Sect. B: Struct. Sci.* **1985**, *41*, 244−247.
(16) (a) Addison, A. W.; Rao, T. N.; Reedijk, J.; van Rijn, J.; Verschoor, G. C. *J. Chem. Soc., Dalton Trans.* **1984**, 1349−1356. (b) Alvarez, S.; Alemany, P.; Casanova, D.; Cirera, J.; Llunell, M.; Avnir, D. *Coord. Chem. Rev.* **2005**, *249*, 1693−1708.
(17) Bartolomé, J.; Filoti, G.; Kuncser, V.; Schinteie, G.; Mereacre, V.; Anson, C. E.; Powell, A. K.; Prodius, D.; Turta, C. *Phys. Rev. B: Condens. Matter Mater. Phys.* **2009**, *80*, 014430.

DOI: 10.1021/acs.inorgchem.5b01179
Inorg. Chem. 2015, 54, 7555−7561